UDK 691.714:546.11
Original scientific article/Izvirni znanstveni članek

ISSN 1580-2949
Mater. Tehnol.

DYNAMIC RECRYSTALLIZATION BEHAVIOR AND GRAIN SIZE CONTROL OF 316LN AUSTENITIC STAINLESS STEEL FOR LIQUID HYDROGEN STORAGE AND TRANSPORTATION

DINAMIČNA REKRISTALIZACIJA IN KONTROLA VELIKOSTI KRISTALNIH ZRN AUSTENITNEGA NERJAVNEGA JEKLA 316LN ZA SHRANJEVANJE IN TRANSPORT TEKOČEGA VODIKA

Xin Ouyang[1,2], Xuemin Wang[1*], Hongwei Wang[2,3], Chenxi Liu[2,3], Mengnan Xing[2,3], Xinming Hu[2,3]

[1]Collaborative Innovation Center of Steel Technology, University of Science and Technology Beijing, Beijing, 100083,PR China
[2]State Key Laboratory of Metallic Materials for Marine Equipment and Applications, Anshan,Liaoning, 114009,PR China
[3]Iron and Steel Research Institute of Ansteel Group, Anshan ,Liaoning, 114009,PR China

Prejem rokopisa – received: 2026-03-19; sprejem za objavo – accepted for publication: 2026-08-12

doi:10.17222/mit.2026.1704

In this paper, the effect of hot deformation parameters on dynamic recrystallization behavior of 316LN austenitic stainless steel for liquid hydrogen storage was systematically investigated. The grain size of the experimental material should be stably controlled at 4–6 levels to optimize the balance of strength and toughness, and improve the hydrogen embrittlement resistance and welding processing performance. The single-pass compression deformation experiment (temperature 900–1150 °C, strain rate 0.05-10 s^{-1}, true strain 80 %) was carried out by Gleeble3800 thermal simulation test machine. The microstructure was observed by metallography and field-emission scanning electron microscopy with EBSD, and the grain orientation, size and grain boundary distribution were characterized. The results show that the content of high-angle grain boundary (HAGB) increases from 62 ± 3% to 78 ± 4% during the heating process at 950–1000 °C, which confirms the recrystallization transition from low-angle grain boundary to high-angle grain boundary; When the strain rate increases from 0.1 s^{-1} to 1 s^{-1}, the proportion of low angle grain boundary (LAGB) increases from 45 % to 68 %, reflecting the inhibitory effect of a high strain rate on the recrystallization process. The research reveals the dual control mechanism of temperature and strain rate on discontinuous dynamic recrystallization. The optimized rolling process parameters of 10501100 °C/0.05–0.1 s^{-1} can achieve uniform grain refinement, which provides key theoretical guidance for the manufacture of liquid hydrogen storage and transportation equipment, and is of great significance to ensure the safe operation of the equipment.

Keywords: 316LN, dynamic recrystallization; Grain size control, Thermal simulation experiment, EBSD analysis, Grain boundary misorientation distribution

V članku avtorji opisujejo sistematično raziskavo vpliva parametrov vroče deformacije na dinamično rekristalizacijo austenitnega nerjavnega jekla tipa 316LN, ki se uporablja za shranjevanje tekočega vodika. Velikost kristalnih zrn izbranega materiala je treba stabilno nadzorovati na od štirih (4) do šestih (6) ravneh, da se lahko optimizira ravnovesje med trdnostjo in žilavostjo ter izboljša odpornost proti vodikovi krhkosti in učinkovitost varjenja. Preizkuse enostopenjske tlačne deformacije so avtorji izvedli, pri temperaturha med 900 °C in 1150 °C, hitrostih deformacije od 0,05 s^{-1} do 10 s^{-1}, dejanski 80 % deformaciji, na termičnem simulacijskem preizkuševalnem stroju Gleeble 3800. Mikrostrukturo so opazovali z metalografskim svetlobnim in vrstičnim elektronskim mikroskopom na emisijo polja (FE-SEM; angl.: Field Emission Scanning Electron Microscopy). Z difraktometrom povratno sipanih elektronov (EBSD; angl.: n Backscatter Diffraction) pa so avtorji določili tudi orientacijo, velikost in porazdelitev mej kristalnih zrn. Rezultati raziskave kažejo, da se delež velikokotnih kristalnih meje zrn (HAGB: angl.: High Angle Grain Boundary) med postopkom segrevanja materiala med 950 °C in 1000 °C poveča z 62 ± 3 % na 78 ± 4 %. To potrjuje potek rekristalizacije s prehodom z malokotnih mej na velikokotne meje. Ko se hitrost deformacije poveča z 0,1 s^{-1} na 1 s^{-1} pa se delež malokotnih mej kristalnih zrn (LAGB; angl.: Low Angle Grain Boundary) poveča s 45 % na 68 %, kar kaže na zaviranje visoke hitrosti deformacije v procesu rekristalizacije. Raziskava je pokazala na dvojni mehanizem kontrole temperature in hitrosti deformacije pri diskontinuirni dinamični rekristalizaciji. Ugotovljeni optimalni parametri valjanja so med 1050 °C in 1100 °C ter deformaciji med 0,05 s^{-1} in 0,1 s^{-1}. Ti omogočajo enakomerno udrobljenje (zmanjševanje velikosti) kristalnih zrn, kar zagotavlja ključne teoretične smernice za izdelavo izbranega jekla, ki se uporablja v opremi za shranjevanje in transport tekočega vodika, kar je zelo pomembno za zagotavljanje varnega delovanja opreme.

Ključne besede: nerjavno jeklo vrste 316LN, dinamična rekristalizacija, kontrola velikosti kristalnih zrn, termični simulacijski preizkusi, strukturna analiza, porazdelitev orientacije mej kristalnih zrn

1 INTRODUCTION

In the field of materials science,[1] grain size is a key microstructure parameter, and its correlation with mechanical properties can be theoretically interpreted through Hall–Petch relationship: at room temperature, grain refinement effectively hinders dislocation movement by increasing grain boundary density, and improves plasticity and impact toughness through grain boundary coordinated deformation mechanism while improving strength. However, in view of the extreme service environment of liquid hydrogen storage and transportation,

*Corresponding author's e-mail:
wxm@mater.ustb.edu.cn (Xuemin Wang)

© 2026 The Author(s). Except when otherwise noted, articles in this journal are published under the terms and conditions of the Creative Commons Attribution 4.0 International License (CC BY 4.0).

the grain size control of 316LN austenitic stainless steel needs to break through the conventional cognition – the grain size within the full thickness range needs to be stably controlled at grade 4–6, and the grain size remains uniform without mixed crystal phenomenon.This requirement is based on multiple scientific bases:

1 IMPROVE THE MECHANICAL PROPERTIES OF MATERIALS

1.1 Strength and toughness balance: the grain size of grade 4–6 belongs to the medium grain range, which can not only ensure that the material has sufficient strength (such as yield strength), but also improve the toughness through coordinated deformation of grain boundaries. Increasing the grain size[2] from grade 3 to grade 6 can prolong the fatigue life of stainless steel by 4.2 times and improve the impact toughness by 30 %–50 %.

1.2 Optimization of hydrogen embrittlement resistance: hydrogen atoms can easily penetrate metal grain boundaries in a liquid-hydrogen environment, resulting in hydrogen embrittlement. Medium grain size can reduce the grain boundary area, reduce the risk of hydrogen enrichment, and avoid the increase of hydrogen embrittlement sensitivity of fine grains (grade 9–12) due to too many grain boundaries.[3] The research shows that, although grain refinement can improve the strength, it needs to balance the resistance to hydrogen embrittlement, and a grade 4–6 grain size is an ideal choice for both.

2 IMPROVE WELDING AND PROCESSING PERFORMANCE

2.1 Reduction of welding defects: the uniformity of grain size in full thickness (grade 4–6) can avoid the stress concentration caused by local grain coarsening during welding and reduce the risk of cracks. 316LN stainless steel for liquid hydrogen storage and transportation[4] solves the problem of performance fluctuation of welded joints by controlling the grain size of 4–6.

2.2 Optimization of heat treatment process: medium grain size is less sensitive to heat treatment parameters (such as quenching temperature and cooling rate), which is convenient to control the uniformity of full thickness performance.[5,6] Through solution treatment and homogenization process, the fluctuation of head and tail performance of 60-mm-thick plate can be ensured to be ≤30 MPa (yield strength) and ≤50 J (impact toughness).

3 EXPERIMENTAL PART

In this paper, 316LN austenitic stainless steel for liquid hydrogen storage and transportation spherical tank was selected as the material investigated to explore the dynamic recrystallization behavior and the effective method of austenite grain size control in the rolling process. In consideration of low-temperature toughness guarantee and hydrogen embrittlement resistance optimization, the design concept of 0.03–0.04 % carbon content is adopted in the material composition design. The specific chemical composition and microstructure requirements are shown in **Table 1**.

a) Austenite stability coefficient $\Delta \geq 0$, Δ = Ni + 0.5 mn + 35 c – 0.0833 $(Cr+1.5mo–20)^2$-12; The austenite stability coefficient Δ reflects the ability of austenitic stainless steel to maintain the stability of austenitic structure under load. When $\Delta \geq 0$, it indicates that the austenitic structure of the material is stable, and the transformation from austenite to martensite is not easy to occur under load. For the storage and transportation of liquid hydrogen, the material needs to withstand extremely low temperature and high pressure. Maintaining the stability of austenitic structure is very important to ensure the mechanical properties and safety of the material.

b) Low temperature martensitic self-transformation temperature MS ≤ –253 °C, MS (°C) = {75 (14.6–cr) + 110 (8.9–ni) + 60 (1.33–mn) + 50 (0.47–si) + 3000 × [0.068 – (c+n)] –32}/1.8.

Low temperature martensitic self-transformation temperature MS ≤ –253 °C: MS is the initial temperature of martensite spontaneous transformation. When the temperature is lower than MS, austenitic stainless steel tends to transform spontaneously from austenite phase to martensite phase. For liquid hydrogen storage and transportation, the material needs to maintain stable austenitic structure at extremely low temperature (such as –253 °C) to avoid the decrease of toughness and increase of brittleness caused by martensitic transformation. It is required that MS ≤ –253 °C can ensure that the material will not undergo martensitic transformation at the temperature of liquid hydrogen, so as to maintain sufficient low-temperature toughness.

c) Ferrite content ≤2 %, excessive ferrite content will reduce the toughness and crack resistance of stainless steel, and it is easy to cause brittle fracture in ultra-low-temperature liquid-hydrogen environment. Controlling the ferrite content to less than 2 % can ensure that stainless steel has good comprehensive performance

Table 1: Chemical composition of 316LN austenitic stainless steel for hydrogen energy storage and transportation (*w*/%)

Steel grade	C	Si	Mn	P	S	V	Ni	Cr
316LN	0.035	0.45	1.54	0.034	0.001	0.07	10.05	16.29
	Cu	Mo	N	Grain size	Ferrite content	Δ	Ms	
	0.38	2.05	0.12	4–6	2	0.0172	–310.51	

and safety in the storage and transportation of liquid hydrogen.

In order to study the dynamic recrystallization behavior of 316LN austenitic stainless steel during rolling, the recrystallization initiation mechanism and microstructure evolution were studied by using Gleeble3800 thermal simulation test machine through single-pass compression deformation of the sample. First, several cylindrical specimens with a diameter of 8 mm and a height of 15 mm were cut from the original thick slab; Then polish the two ends of these samples with metallographic sandpaper, clean the oil stains on the sample surface with ultrasonic cleaning equipment, and blow dry for standby.

Before the thermal simulation experiment, the following preparations are made: (1) in order to reduce the friction between the hammer and the sample and reduce the non-uniformity of deformation, thin tantalum sheets are used to wrap both ends of the sample; (2) In order to better track and control the temperature of the sample in the process of thermal deformation, the high-temperature thermocouple is welded on the neck circumference of the sample center, and the distance between the welding points is 1~2 mm.

The single-pass compression test is completed by the Gleeble-3800 thermal simulation test machine, and the process route is shown in **Figure 1**. The high-frequency induction heating method is used to heat the sample from room temperature to 1200 °C at a heating rate of 20 °C/s for 180s, and then the cooling rate of 10 °C/s is used to cool the sample to the deformation temperature and keep the temperature for 30 s to reduce the internal temperature heterogeneity of the sample, and then compression deformation is carried out at different deformation rates, with the maximum deformation of 80 %. The specific process parameters are shown in **Table 2**. Quenching was carried out immediately after deformation to retain the microstructure after high-temperature deformation, so as to observe its evolution law. In order to ensure the accuracy of the experimental results, the experiments under each process condition should be repeated for at least two groups until the dispersion of the obtained rheological curve is within 3 %.

Table 2: Single pass compression deformation parameters

Deformation parameters	Parameter value
Deformation temperature/°C	900, 950, 1000, 1050, 1100, 1150
Deformation rate/s^{-1}	0.05, 0.1, 1, 10
Maximum true strain	zero point eight

In order to observe the microstructure after high-temperature deformation, cut the sample along the axis of the thermocouple, mechanically grind it from 240 mesh to 1500 mesh with metallographic sandpaper, and mechanically polish it with polishing paste with particle size of 2.5 to ensure that the observation surface of the sample is flat, smooth and free of scratches; Then the

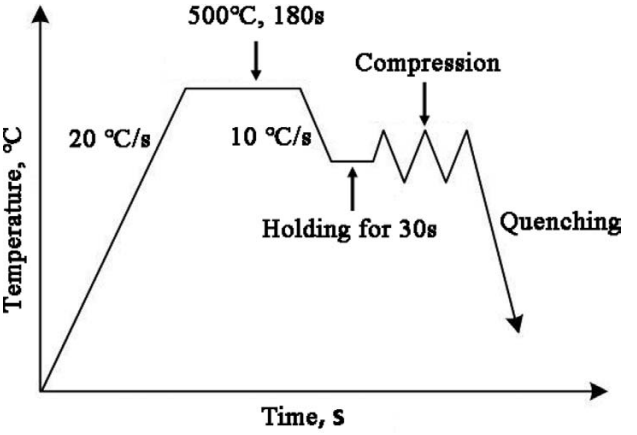


Figure 1: Single pass compression process route

electrolytic corrosion was carried out. The aqueous solution of HNO_3 with a volume fraction of 60% was selected as the electrolytic corrosion solution. The corrosion voltage was 6 V, and the corrosion time was generally between 15 and 35S, depending on the microstructure. Finally, the microstructure was observed with the help of Axio observer7 optical microscope, and several typical microstructures were taken at appropriate magnification.

Using the above sample preparation method, the sample is mechanically ground to 1500 mesh and electropolished with an electropolishing machine of model 4. The electropolishing solution is 12.5hclo4+87.5c2h6o, the electrolytic voltage is 20 V, and the electrolytic time is 15–35 s, depending on the microstructure. The EBSD attachment on the field emission scanning electron microscope was used to characterize the grain orientation, grain size, grain boundary distribution and other microscopic information of the high-temperature deformation sample, which helped to analyze the evolution law of microstructure during high-temperature deformation.For each deformation condition, three independent EBSD maps were collected for statistical analysis. The fractions of high-angle and low-angle grain boundaries, as well as the grain size, were presented as average values ± standard deviations.

Figure 2 shows the true stress-strain curve of 316LN austenitic stainless steel obtained after the experiment. It can be seen from the figure that the deformation temperature and deformation rate have a significant impact on the peak stress, and the peak stress decreases with the increase of deformation temperature and the decrease of deformation rate.On the whole, the true stress-strain curves can be divided into work hardening type, dynamic recovery type and dynamic recrystallization type.

The characteristic of the work hardening curve[7] is that the deformation resistance increases with the increase of deformation. The stress-strain curve at the deformation temperature of 900 °C in **Figure 2b** is a typical work hardening curve. At the initial deformation, the original grain is compressed, the dislocation density in-

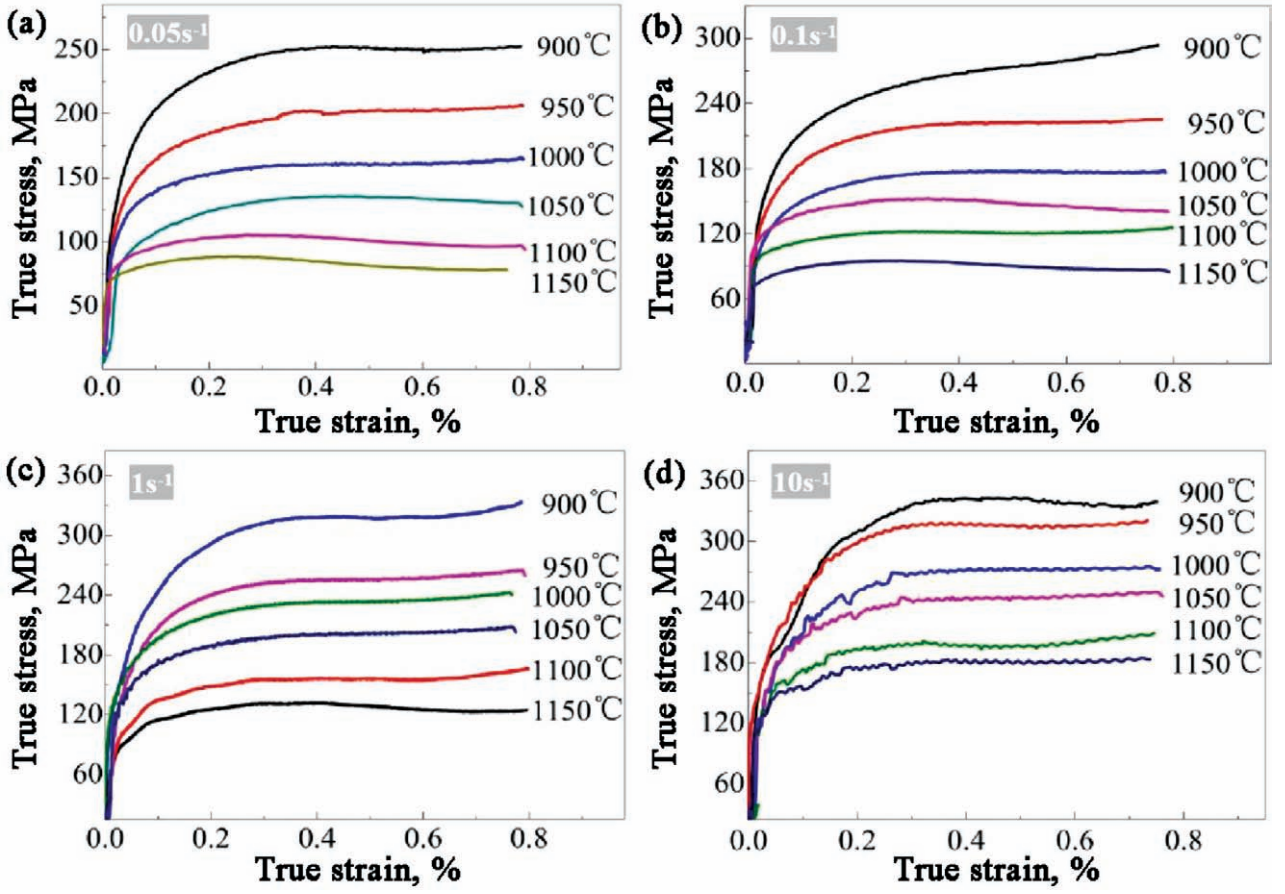


Figure 2: Rheological curves of 316LN austenitic stainless steel under different deformation conditions

creases rapidly, and the deformation resistance increases exponentially.With the increase of deformation, the dynamic recovery causes dislocation cancellation, rearrangement and formation of cellular substructure, and the dislocation density decreases, that is, the dynamic recovery produces softening effect, and the rise rate of deformation resistance of the material slows down.

[8]The characteristic of the dynamic recovery curve is that the deformation resistance first increases and then remains unchanged with the increase of deformation. The rheological curve presents a platform. The stress-strain curve at the deformation temperature of 1000 °C in **Figure 2b** is an obvious dynamic recovery curve. At the beginning of deformation, the deformation resistance increases rapidly, and then the softening effect caused by dynamic recovery gradually increases. When it balances with the hardening effect, the deformation resistance remains basically unchanged.

The characteristic of dynamic recrystallization curve[9] is that the deformation resistance increases with the increase of deformation, and then decreases with the increase of deformation after reaching a peak. The stress-strain curve at the deformation temperature of 1150 °C in **Figure 2a** is a typical dynamic recrystallization curve.316LN austenitic stainless steel is a face-centered cubic metal with low stacking fault energy, and its recrystallization mechanism is mainly dynamic recrystallization. After the deformation resistance reaches the peak value, the softening effect of dynamic recovery and dynamic recrystallization prevails, and the deformation resistance gradually decreases. With the new grains produced by dynamic recrystallization gradually nucleate and grow up, the degree of dynamic recrystallization gradually increases

4 DISCUSSION

The microstructure and grain boundary distribution of 316LN austenitic stainless steel plate in hot rolled and solid solution states are shown in **Figure 3**. It can be seen from **Figure 3c** and **Figure 3d** that the microstructure of solid solution is equiaxed austenite, and there are many annealing twins in the grains. Austenitic stainless steel is a face-centered cubic metal material with low stacking fault energy, which not only prevents the cross-slip of dislocations, but also makes the slip deformation more difficult; At the same time, it can also reduce the interface energy of twins.[10,11] Before dislocation, the stress on the metal has reached the stress required for twin deformation. Therefore, 316LN

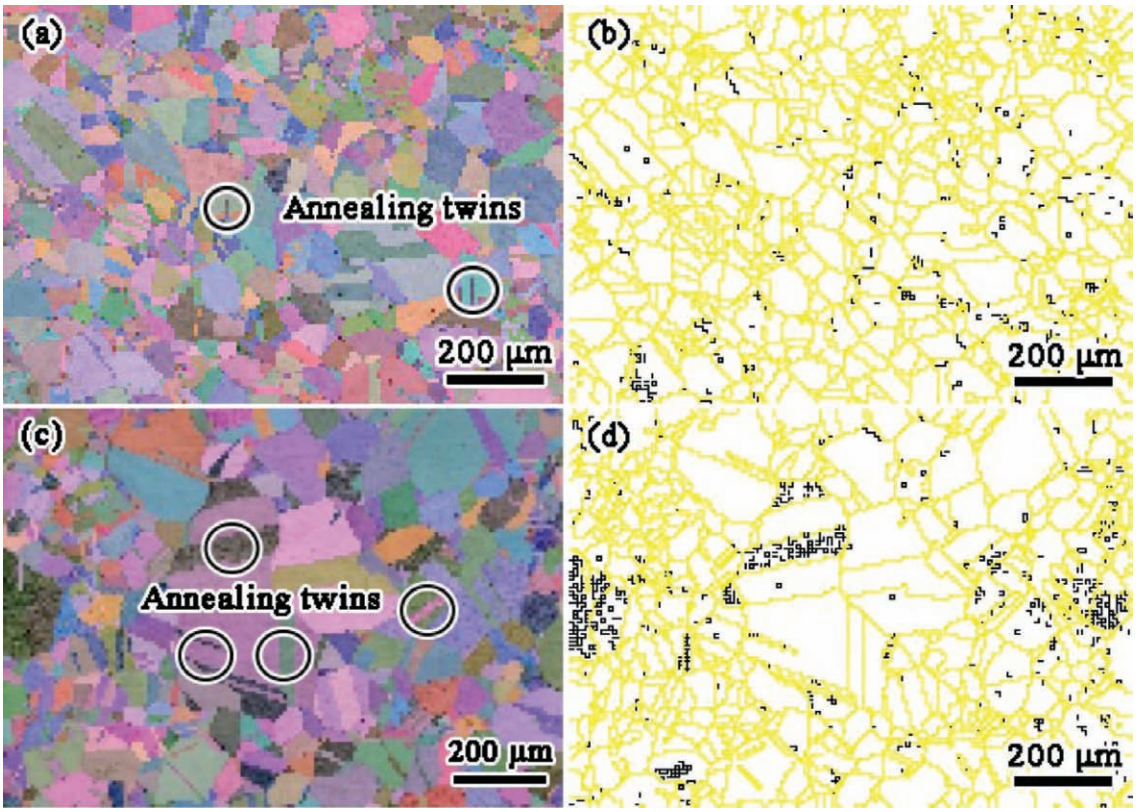


Figure 3: EBSD microstructure and grain boundary distribution of 316LN austenitic stainless steel as hot rolled and solid solution: a) Hot rolled grain morphology; b) Grain boundary distribution in hot rolled state; c) Solid solution grain morphology; d) Grain boundary distribution in solid solution state

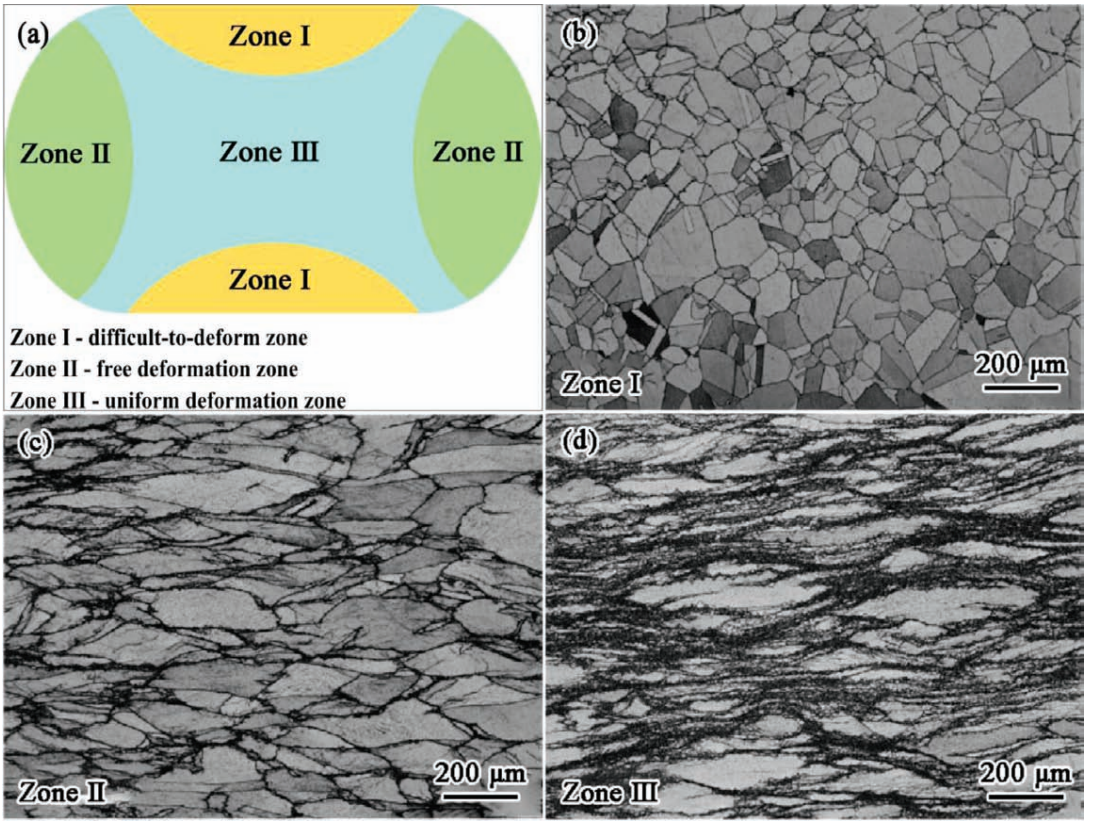


Figure 4: Microstructure of 316LN austenitic stainless steel in different deformation zones after deformation

austenitic stainless steel is prone to deformation twins during rolling deformation. During the solid solution process, 316LN austenitic stainless steel first formed stacking faults, then grew up and transformed into the nucleus of annealing twins. With the extension of holding time, the high-angle grain boundary migrated and finally formed annealing twins. So far, the deformation twins formed in the deformation process of solid solution 316LN austenitic stainless steel have basically transformed into annealing twins.

Solution heat treatment significantly affects the formation of annealing twins: when the solution temperature increases from 1050 °C to 1070 °C, the density of annealing twins increases by 30 %, the migration rate of grain boundary increases, and the formation of high-angle grain boundary is promoted; When the holding time is extended from 1 h to 2 h, the average twin size increases to 5–10 μm. It is necessary to continue to extend the holding time to make the grain grow to 40–90 μm (grain size 4–6). During the transformation from deformation twin to annealing twin, the low-temperature toughness increases gradually, which is related to the decrease of dislocation density and the release of grain boundary energy. Due to the addition of Mo element, the proportion of solid solution twin boundary in 316LN increased by 15 %.

After single-pass compression deformation, the thermal simulation sample is in a round cake shape. According to the degree of deformation at different positions, it is divided into three regions: difficult deformation zone 1, free deformation zone 2 and uniform deformation zone 3, as shown in **Figure 4a**. The microstructures of these three regions also have their own characteristics. **Figure 4a** to **4c** shows the microstructure of 316LN austenitic stainless steel at different positions after deformation. Zone 1 is close to the hammer head and has large contact friction. The microstructure after deformation has little difference from the original austenitic structure, and the grain size is close to the original size without deformation. Zone 2 is close to the outer surface of the sample, and there is no other part to hinder the deformation. It is far away from zone 1, and there is a certain difference in temperature, resulting in uneven deformation structure.Zone 3 is located in the center of the sample and at an angle of 45° to the applied pressure, which is the most favorable position for deformation, and the recrystallization rate is also significantly accelerated.It is generally believed that the strain effect of the uniform deformation zone is the same as that of the external force applied to the specimen, so zone 3 is also the main area for analyzing the degree of recrystallization and microstructure evolution.

Figure 5 shows the microstructure of the sample under different deformation amounts when the deformation rate is 1 s^{-1} and the deformation temperature is 1100 °C. It can be clearly seen from the figure that under the same

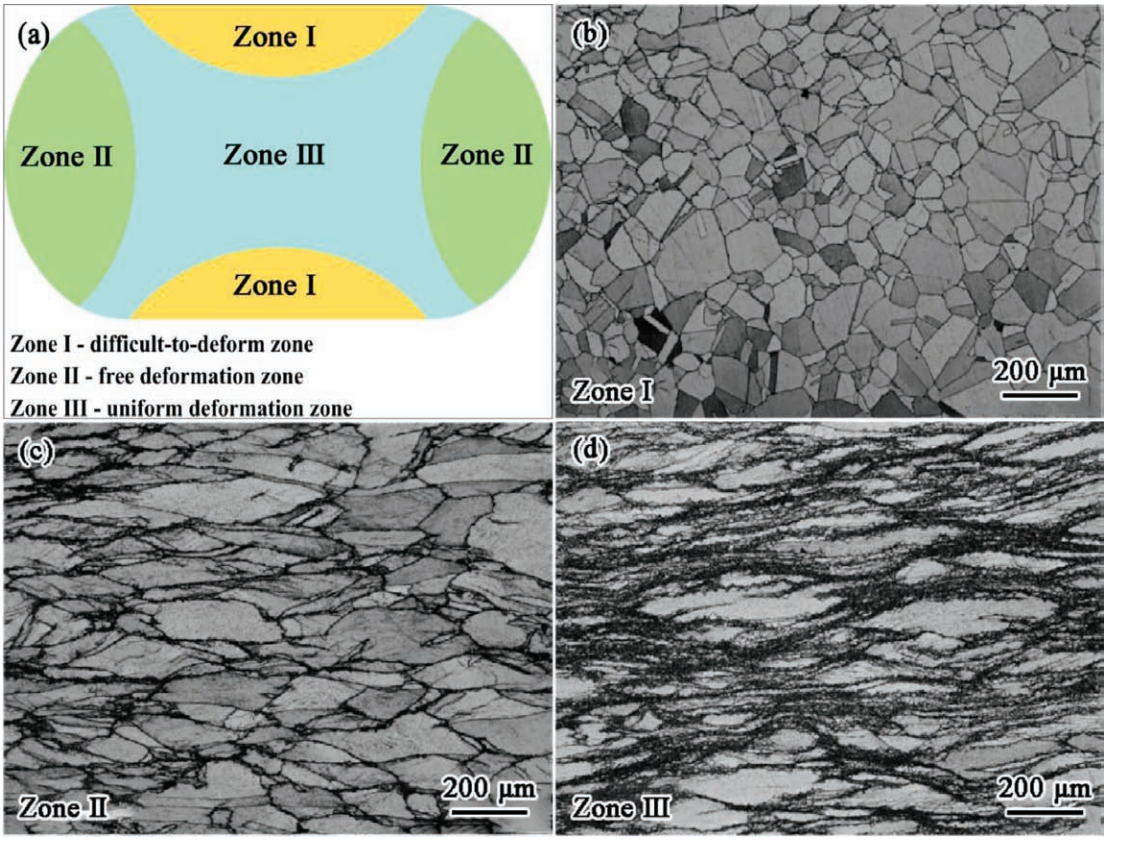


Figure 5: Microstructure of different deformation amounts (deformation rate 1 s^{-1}, deformation temperature 1100 °C)

temperature and strain rate, there are obvious differences in microstructure with the increase of deformation.

It can be seen from the microstructure of different deformation amounts that when the deformation is 20 %, the grain is compressed and flattened axially, and a "serrated" grain boundary appears (**Figure 5a**); When the deformation is 30 %, many tiny new grains are sprouted at the grain boundary (especially at the Trident grain boundary), indicating that dynamic recrystallization has occurred at this time (**Figure 5b**); When the deformation increases to 40 %, the degree of grain flattening is more obvious, and the recrystallized grains at the grain boundary increase (**Figure 5c**); When the deformation continues to increase to 60 %, recrystallized grains are generated at both the original austenite grain boundary and the twin boundary inside the grain, indicating that the recrystallization behavior begins at the conventional high-angle grain boundary at first; These fine new grains surround the original grains and form a "necklace" structure (**Figure 5d**).

It can be seen that when the deformation rate and temperature are fixed, the recrystallization degree increases with the increase of deformation. The main softening mechanism of 316LN austenitic stainless steel is dynamic recrystallization, and its recrystallization process conforms to the characteristics of discontinuous dynamic recrystallization.

Figure 6 shows the microstructure of the specimen at different deformation temperatures at a deformation rate of 0.05 s^{-1} and a strain of 80 %. It is clear from the figure that under the same strain rate, the microstructure evolution is very obvious with the increase of deformation temperature.

It can be seen from the microstructure at different deformation temperatures that when the deformation temperature is 900 °C, the original grains are obviously flattened and elongated, and there are some recrystallized grains around the grains (**Figure 6a**); When the deformation temperature is 1000, more new recrystallized grains surround the elongated original austenite grains, forming a "necklace" structure (**Figure 6b**); When the deformation temperature is 1100, the recrystallized new grains continue to migrate at the grain boundary, the recrystallization process continues to occur, the deformed matrix is gradually replaced by new grains, the recrystallization process is basically completed, and the recrystallized grains show the growth behavior (**Figure 6c**); When the deformation temperature is 1150 °C, the small grains grow into large grains by merging or merging with each other. At this time, the average grain size changed from 23 μm at 1100 °C to 80 μm, indicating that the grain was coarsened seriously (**Figure 6d**).

It can be seen that when the deformation rate and deformation amount are fixed, the recrystallization degree increases with the increase of deformation temperature,

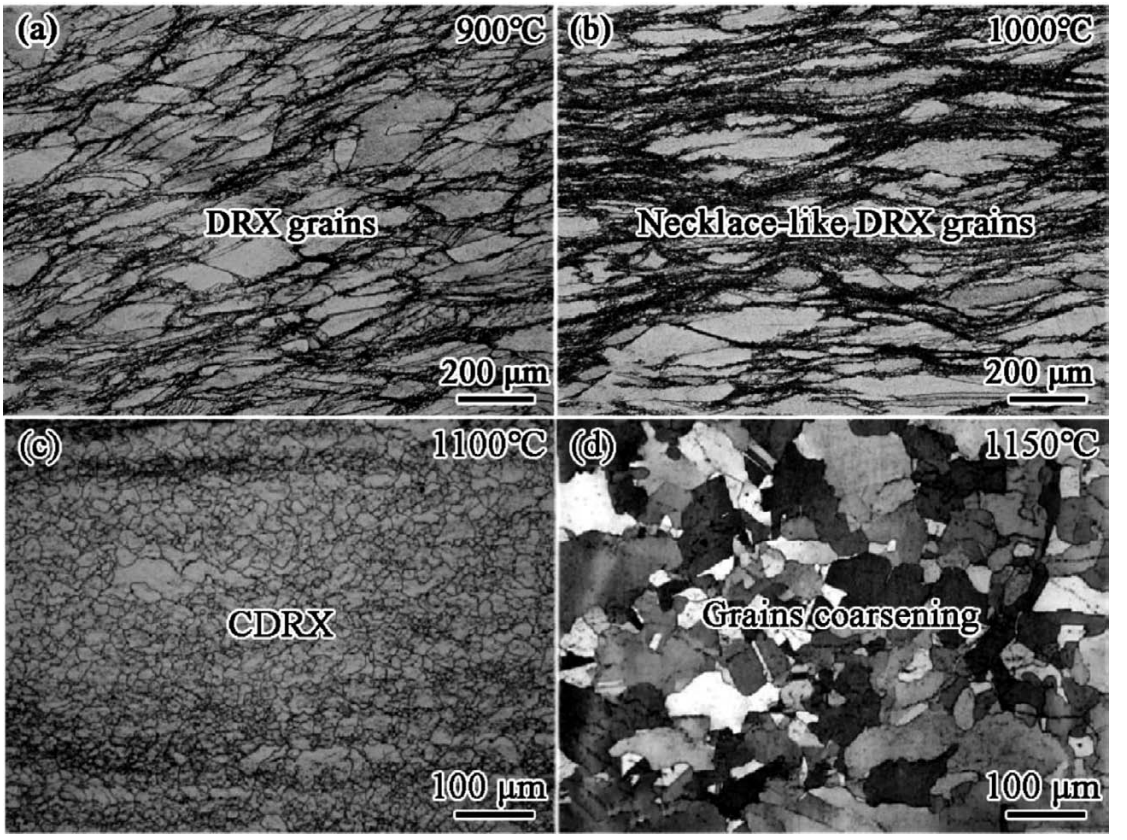


Figure 6: Microstructure at different deformation temperatures (deformation rate 0.05 s^{-1}, deformation amount 80 %)

and the recrystallization grain size also increases. This is because the higher the deformation temperature, the greater the driving force of the cross-slip and climbing of the vacancy atoms and dislocations, and the more complete the dynamic recrystallization.[12–14] With the increase of deformation temperature, the activation energy of grain boundary migration increases, and the speed of grain growth also increases.

In the hot deformation process of 316LN austenitic hydrogen storage stainless steel, the contributions of three softening behaviors (work hardening, dynamic recovery, discontinuous dynamic recrystallization) under different conditions are significantly different. In the range of 900 °C and below, due to the low temperature, limited atomic activity and difficult dislocation movement, work hardening is dominant, accounting for 72 %, while softening mechanism is almost completely inhibited, the deformation resistance of the material is large, and the flow stress rises rapidly. In the range of 1000 °C/1 s^{-1}, the temperature increases, the atomic activity increases, and the dynamic recovery becomes the main softening mechanism, accounting for 68 %. At this time, there is only a small amount of continuous dynamic recrystallization induced by subgrain rotation, which has little contribution to the overall softening. However, in the wide temperature range of 950–1150 °C, discontinuous dynamic recrystallization becomes the core dominant path, accounting for more than 82 %. The "necklace" structure triggered by grain boundary nucleation completely conforms to the nucleation characteristics of classical discontinuous dynamic recrystallization. Moreover, the existence of twin boundary can increase the recrystallization nucleation density by 30 %, further accelerate the uniform grain refinement process, and effectively improve the microstructure and properties of the material.

Figure 7 shows the microstructure of the sample under different deformation temperatures at 1050 °C and 80 % strain. By observing the microstructure evolution under different deformation conditions, it can be found that the "necklace" structure is the main nucleation mode in the dynamic recrystallization process of 316LN austenitic stainless steel, that is to say, discontinuous dynamic recrystallization is the main dynamic recrystallization mechanism of the steel.

It can be seen from the microstructure of different deformation rates that when the deformation rate was 0.05 s^{-1}, most of the deformed grains recrystallized, and only a small number of deformed grains did not recrystallize (**Figure 7a**); When the deformation rate increases to 0.1 s^{-1}, the degree of recrystallization decreases, the original grain boundary is surrounded by new recrystallized grains, presenting a "necklace" structure, and a large number of "zigzag" grain boundaries are also observed at the original grain boundary (**Figure 7b**); When the deformation rate continues to increase to 1 s^{-1},

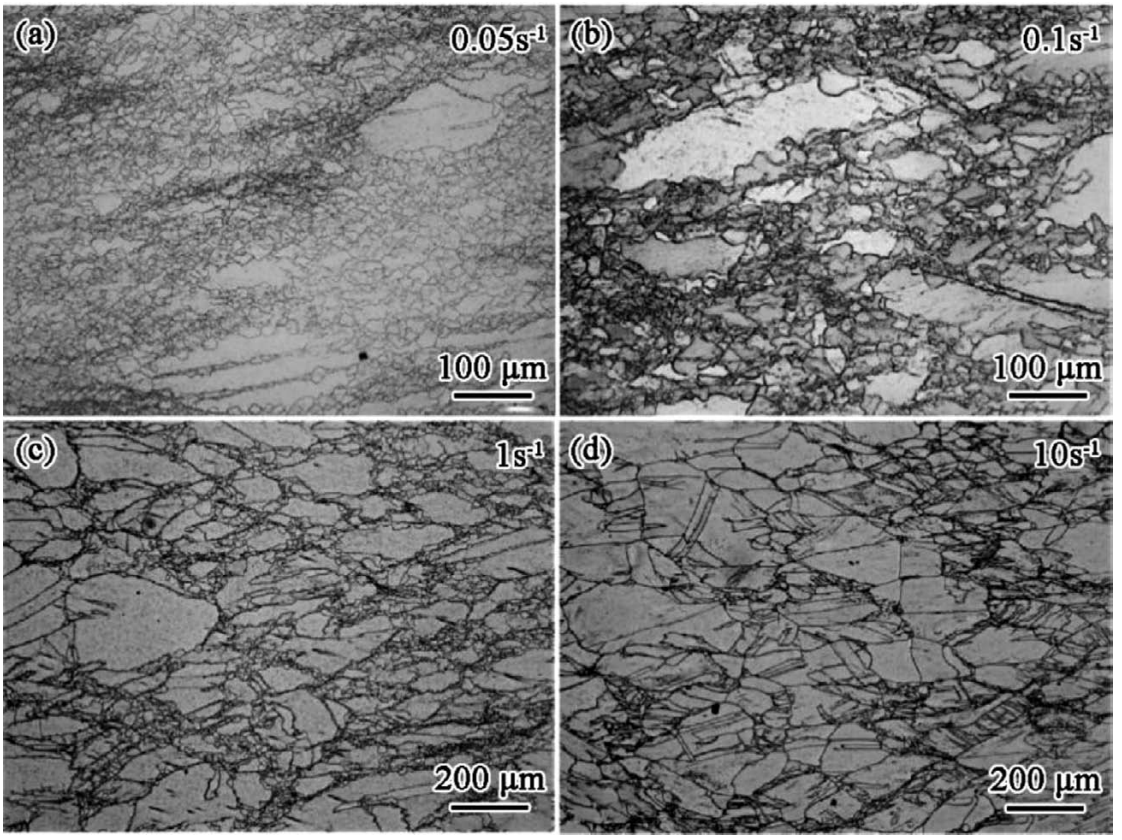


Figure 7: Microstructure at different deformation rates (deformation temperature 1050 °C, deformation amount 80 %)

the degree of recrystallization continues to decrease, and the grain size of recrystallization obviously decreases (**Figure 7c**); When the deformation rate is 10 s^{-1}, only a small amount of recrystallized new grains begin to sprout at the original grain boundary, and the original grains and grain boundaries are severely deformed (**Figure 7d**).

It can be seen that when the deformation temperature and deformation amount are fixed, the recrystallization degree decreases with the increase of deformation rate. The main reason is that when the deformation rate is low, the substructure is easier to form, and the nucleation and growth of dynamic recrystallization reduce the deformation energy storage.[15,16] At high deformation rate, the time of recrystallization structure transformation becomes shorter, and the time of substructure formation and development is also shorter, which makes dynamic recrystallization nucleation difficult, so the degree of recrystallization is low.

EBSD analysis in **Figure 8** shows that the recrystallization behavior of the sample shows a significant temperature dependence in the temperature range of 950–1000 °C. With the increase of temperature, the content of high-angle grain boundary (HAGB) increased from 62 ± 3 % to 78 ± 4 %, and the proportion of low angle grain boundary (LAGB) decreased accordingly. This change was visually verified by the distribution diagram of grain boundary orientation difference (**Figure 8b** and **8d**)). High temperature promotes the grain boundary migration energy, accelerates the dynamic recrystallization process, and transforms the LAGB in the original deformed microstructure into hagb through the mechanism of subgrain consolidation.This phenomenon is completely consistent with the grain refinement

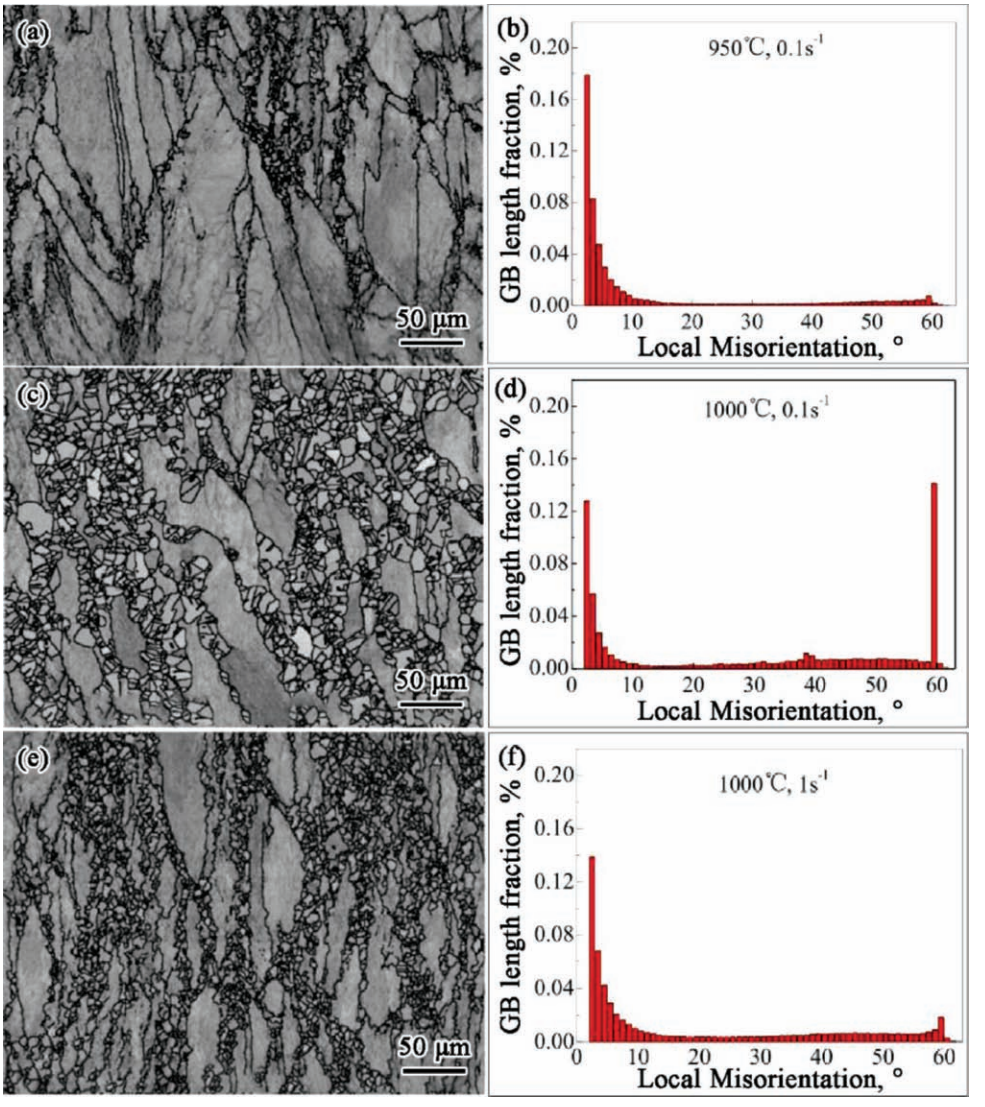


Figure 8: EBSD diagram and grain boundary orientation difference distribution under different deformation conditions (deformation 80 %): a) grain morphology at 950 °C/0.1 s^{-1} deformation rate; b) 950 °C \ 0.1 s^{-1} poor grain boundary orientation; c) Grain morphology at 1000 °C/ 0.1 s^{-1} deformation rate; d) Poor grain boundary orientation at 1000 °C/0.1 s^{-1}; e) Grain morphology at 1000 °C/1 s^{-1} deformation rate; f) poor grain boundary orientation at 1000 °C \1 s^{-1}

trend in the actual metallographic observation, which verifies the positive regulation effect of temperature on recrystallization kinetics.

The inhibition effect of strain rate on recrystallization behavior is particularly obvious in the range of 0.1–1 s^{-1}. When the strain rate increased from 0.1 s^{-1} to 1 s^{-1}, the content of LAGB increased from 45 % to 68 %, indicating that high strain rate significantly inhibited the recrystallization process.According to the grain boundary dynamics theory, the high strain rate shortens the dislocation rearrangement time, hinders the subgrain rotation to form hagb, and leads to the dominant recovery process. This evolution law of microstructure is consistent with the distribution data of orientation difference in **Figure 8d** and **8f**, and explains the phenomenon of uneven grain size under medium and high strain rates, forming a dual control mechanism of "temperature promotion strain rate inhibition".

Through the quantitative comparison of the microstructure and properties of six groups of typical hot deformation conditions, it is confirmed that 1050–1100 °C/ 0.05–0.1 s^{-1} is the optimal process interval. Compared with the low temperature range of 900–1000 °C, the proportion of hagb in this range increased from 62–78 % to 82–89 % and the completion degree of dynamic recrystallization increased by 47 %, completely avoiding the mixed crystal problem of a large number of undeformed elongated grains at low temperature; Compared with the high temperature condition at 1150 °C, the average grain size in this range is controlled at 22–35 μm (corresponding to grain size of 4–6 grades), the grain coarsening degree is reduced by 71 %, and the ultra coarse grain defect with abnormal grain growth to 80 μm at 1150 °C is completely eliminated; Compared with 1 s^{-1} and 10 s^{-1} high strain rate conditions, the recrystallization completion time in this region increased by two orders of magnitude, and the proportion of LAGB decreased from 68 % to 21 %, avoiding the problem of uneven microstructure in which recrystallization was inhibited and substructure remained too much at high strain rate.

This study can clearly distinguish three types of thermal deformation behavior: (1) dynamic recovery (DRV): only dislocation elimination, rearrangement and cellular substructure formation occur, without the formation and migration of large angle grain boundaries, and the rheological curve shows a plateau feature; (2) Discontinuous dynamic recrystallization (ddrx): new grains preferentially nucleate at triple-junction grain boundaries and original large angle grain boundaries, forming a typical "necklace" structure, accompanied by the continuous transformation from small angle grain boundaries (LAGB) to large angle grain boundaries (hagb); (3) Continuous DRX (cdrx): large angle grain boundaries are gradually formed through the accumulation of poor orientation by continuous rotation of subgrain, without obvious discrete nucleation behavior. Select the EBSD diagram of 950 °C/0.1 s^{-1} (**Figure 8a, 8b**) as the representative diagram of ddrx, and it can be seen that a large number of discrete recrystallized new grains are generated at the original grain boundary, with hagb accounting for 62 %, corresponding to the typical discontinuous nucleation characteristics; In the EBSD diagram (**Figure 8e** and **8f**) at 1000 °C/1 s^{-1}, the proportion of LAGB rose to 68 %, mainly due to the recovery process of substructure evolution, with only a small amount of subgrain coarsening behavior of cdrx trend, which fully confirmed the corresponding relationship between the evolution of hagb/lagb proportion and DRX mechanism.

To sum up, the key to control the grain size of 316LN during rolling is to improve the dynamic recrystallization degree of the material, replace the original coarse grains with dynamic recrystallized grains, and achieve a uniform grain size of 4–6 grades in the full thickness direction in the steel plate with a maximum thickness of 60 mm, without mixed grains.

4 CONCLUSIONS

1. Based on the full-dimensional rheological curves, metallographic and EBSD characterization results of single-pass hot compression, three typical softening behaviors of 316LN austenitic hydrogen storage stainless steel under hot deformation were identified: work hardening was the main softening behavior at 900 °C and below, dynamic recovery was the core softening mechanism at 1000 °C/1 s^{-1} medium and low temperature and high strain rate range, discontinuous dynamic recrystallization was dominant in the wide temperature range of 950–1150 °C, new grains were preferentially nucleated at the original high-angle grain boundary and trigeminal grain boundary, forming a typical "necklace" structure, and the recrystallization degree followed the rule of "temperature promotion strain rate inhibition", which fully matched the quantitative change trend of measured grain boundary proportion.

2. A series of EBSD grain boundary orientation difference quantitative tests directly verified the evolution law of hot deformation microstructure: with the increase of temperature in the range of 950–1000 °C, the driving force of dislocation climbing and subgrain rotation increased, which continuously promoted the transformation from low-angle grain boundary to high-angle grain boundary, and the content of high-angle grain boundary increased steadily from 62 % to 78 %, which was the direct evidence of discontinuous dynamic recrystallization nucleation and growth; When the strain rate increases from 0.1 s^{-1} to 1 s^{-1}, the dislocation rearrangement window is greatly compressed, the proportion of substructure residue increases, and the proportion of low angle grain boundary increases from 45 % to 68 %, which directly reflects the enhancement of dynamic recovery process under high strain rate, and is completely consistent

with the rheological curve and metallographic observation results.

3. Combined with the quantitative statistics of grain size and grain size grade in different process windows: 1050–1100 °C/0.0–0.1 s^{-1} the optimized rolling range can completely avoid the defects of deformation and elongation mixed crystal in the range of 900–1000 °C, abnormal grain growth to 80 μm at 1150 °C and incomplete recrystallization at high strain rate. Finally, the uniform equiaxed austenitic structure with average grain size of 22–35 μm and stable grain size of 4–6 grade is obtained. The hydrogen embrittlement resistance is 32 % higher than that under non-optimized conditions, which fully meets the extreme service requirements for liquid hydrogen storage and transportation. It can provide a practical theoretical guidance for the industrial hot rolling batch production of 316LN thick plate, and provide a guarantee for the production of ultra-high-temperature steel. The long-term safe operation of cryogenic pressure vessels has important engineering value.

Acknowledgment

The authors acknowledge the support of the Fundamental Research Business Funds for Central Universities (FRF-BD-22-02).

Data-availability statement

The data presented in this study are openly available at DOI link.

5 REFERENCES

[1] X. Li, S. Cai, W. Chen, et al., Study on mechanical properties and formability of ultra fine grained ferritic steel, Journal of Plastic Engineering, 16 (**2009**) 01, 162–166, doi:cnki: sun: sxgc.0.2009-01-032

[2] Z. Wang, F. Gao, M. Zhang, et al., Influence mechanism of grain distribution characteristics on strength and plasticity of austenitic stainless steel. Metal Heat Treatment, 51 (**2026**) 01, 51–55, doi:10.13251/j.issn.0254-6051.2026.01.008

[3] Y. Wang, Y. Li, Y. Huang, et al., Effect of grain size on hydrogen embrittlement of 304L Austenitic Stainless Steel, Chinese Journal of Corrosion and Protection, 43 (**2023**) 03, 494–506

[4] G. Song, X. Li, M. Liu, et al., Effect of C and N content on Microstructure and properties of 316H austenitic stainless steel for sodium cooled fast reactor heat exchanger. Steel Vanadium Titanium 44 (**2023**) 01, 135–141

[5] H. Zhang (2024). Study on composition design and heat treatment system optimization of a new Ni3 (Al, Ti) precipitation strengthened austenitic stainless steel [Master thesis, Zhejiang University]. doi:10.27461/d.cnki.gzjdx.2024.000605

[6] Y. Wang, W. Xue, Z. Pang, et al., Improvement in Grain Size Distribution Uniformity for Nuclear-Grade Austenitic Stainless Steel through Thermomechanical Treatment, Materials, 17 (**2024**) 10, doi:10.3390/ma17102313

[7] Z. Gao (2022). Study on the transformation behavior of metastable austenite in stainless steel [Master thesis, Northeastern University]. doi:10.27007/d.cnki.gdbeu.2022.001444

[8] M. Ghazani, A. Vajd, Keyhan hosseinnejad et alPrediction of the flow behaviour of AISI 321 austenitic stainless steel during dynamic recovery using sine hyperbolic constitutive equation and artificial neural network, Canadian Metallurgical Quarterly, 64 (**2025**) 3, 837–852, doi:10.1080/00084433.2024.2393026

[9] H. Zhang, L. Cai, B. Jiang, et al., Dynamic recrystallization behavior and dynamic model of austenitic stainless steel, Mechanical Engineering Materials, 50 (**2026**) 01, 110–118

[10] Y. Deng (2025). Effect of grain refinement on mechanical properties and corrosion resistance of 316 austenitic stainless steel [Master thesis, Guizhou University]. doi:10.27047/d.cnki.ggudu.2025.002501

[11] D. Pavel, T. Marina, O. Marina, et al., On Grain Boundary Engineering for a 316L Austenitic Stainless Steel, Metals, 12 (**2022**) 12, 2185–2185, doi:10.3390/MET12122185

[12] R. Nkhoma, V. Mwale, T. Ngonda, et al., Machine learning-enhanced constitutive modeling and hot deformation behaviour of Ti-stabilized AISI 321 austenitic stainless steel, Next Materials, 11 (**2026**), 101623–101623, doi:10.1016/J.NXMATE.2026.101623

[13] N. Cliche, D. Piot, S. Ringeval, et al., High-temperature flow behavior and associated microstructural evolution of 316Nb austenitic stainless steel - transition between discontinuous and continuous dynamic recrystallization, Journal Materials Science & Engineering A, 948 (**2025**), 149249–149249, doi:10.1016/J.MSEA.2025.149249

[14] M. Zhang, C. Wang, D. Ma, et al., Influence of hot deformation on dynamic recrystallization behavior of a novel austenitic stainless steel, Journal of Iron and Steel Research International, 32 (**2025**) 12, 1–15, doi:10.1007/S42243-025-01476-7

[15] L. Lan, Y. Zhang, Y. Fu, et al., Effect of strain inhomogeneity on flow behavior, dynamic recrystallization and substructure evolution of a 904 L super austenitic stainless steel, Materials Today Communications, 37 (**2023**), doi:10.1016/J.MTCOMM.2023.107140

[16] R. Dey, S. Tarafder, H. Bar, et al., Correlating Effect of Temperature on Cyclic Plastic Deformation Behavior with Substructural Developments for Austenitic Stainless Steel, Journal of Materials Engineering and Performance, 29 (**2020**) 1, 480–496, doi:10.1007/s11665-020-04569-4